Kingdom of Saudi Arabia
Imam Muhammad Ibn Saud Islamic
University (IMSIU)
Faculty of Science - Department of Physics

Study of Longitudinal electron beam dynamics in a compact S-band Standing Wave (SW) Radio-Frequency (RF) Photoinjector (1.5 cell design)

A graduation project submitted to the Department of Physics in partial fulfillment of the requirements for the degree of Bachelor of Science in Applied Physics

by

Al.anoud Dakhilallah Alotaibi

Supervised by

Dr. Muneerah Al-Aqeel

&

Dr. Muath Alkadi

October 3, 2024

Contents

Acknowledgements

Firstly,I would like to express my sincere gratitude to my supervisor Dr. Muneerah Al-Aqeel, I want to express my deepest appreciation for everything you have done for me. Also, my sincere thanks go to Dr. Muath Alkadi for the continuous support of my thesis. In addition, they provided me with an opportunity to join their team as an intern, and who gave access to the laboratory and research facilities. Without their precious support it would not be possible to conduct this research. Besides my supervisors, also would like to express our gratitude to Imam Mohammad Ibn Saud Islamic University (IMAMU) and King Abdulaziz City for Science and Technology (KACST) for giving me the chance to participate in the graduation project at the Nuclear Technologies Institute (NTI) as well as for closely monitoring me throughout the project time. Moreover, my appreciations also goes for the hard question which incited me to widen my research from various perspectives. I thank my fellow lab-mates for the stimulating discussions. Also, I thank my friends in the department of physics. Last but not least, I would like to thank my family: my parents for supporting me spiritually throughout the first year of my BPhys study and my life in general.

Abbreviation and Acronym

SW	Standing Wave
RF	Radi-Frequency
AC	Alternating Current
LINAC	Linear Accelerator
SLAC	Standford Linear Accelerator Center
LCLS	Linac Coherent Light Source
NCRF	Normal Conducting Radio-Frequency
XFEL	X-ray Free-Electron Laser
SCRF	Superconducting Radio-Frequancy
NTI	Nuclear Technologies Institute
KACST	king Abdulaziz City for Science and Technology
Cu	Copper
Pb	Lead
Mg	Magnesium
MHz	Megahertz
GHz	Gigahertz
Kev	Kiloelectronvolt
Mev	Megaelectronvolt
MW	Megawatt
fs	Femtosecond
nC	Nanocoulombs
pC	Picocoulomb
Mv	Megavolt
cm	Centimeter
m	Meter

List of Figures

Abstract

Nowadays, particle accelerators play an important role as powerful engines that speed up tiny charged particles to incredibly high speeds close to the speed of light. These machines are essential in many scientific areas: Understanding the Universe, many medical applications, nuclear Studies, Astrophysics, and Industrial Uses. This research highlights on the longitudinal electron beam dynamics in a compact S-band standing wave radio-frequency photoinjector of 1.5 cell, focusing on the generation and acceleration characteristics of the electron beam under the RF fields. This research clearly examines the intricate interplay between electric fields and their profound impact on the extraction and acceleration mechanisms governing electron beams within accelerator cavities. Through meticulous analysis, we are able to know how variations in electric field strength, under various conditions within the photoinjector setup such as the RF phase, directly affect the efficiency of beam generation, extraction and the subsequent acceleration processes within these specialized cavities. This is carried out with a support of analytical models and simulation program (MATLAB). This study is also unique in the country and provides scientific access and resources for accelerator physicists, experts and researchers.

الملخص

في الوقت الحاضر، تلعب مسرعات الجسيمات دورًا مهمًا كأجهزة ومعدات ضخمة تعمل على تسريع الجسيمات المشحونة إلى سرعات عالية تقترب من سرعة الضوء. هذه المعدات تعتبر ضرورية في العديد من المجالات العلمية فعلى سبيل المثال: فهم الكون، والعديد من التطبيقات الطبية، والدراسات النووية، والفيزياء الفلكية، والاستخدامات الصناعية.

يسلط هذا البحث الضوء على ديناميكيات حزمة الإلكترون المتسارعة طولياً في الحاقن الضوئي والمكون من خلية ونصف ومزود بموجات ثابتة في نطاق اس الترددي ، مع التركيز على خصائص توليد وتسريع حزمة الإلكترون تحت حقول التردد اللاسلكي.

كما يدرس هذا البحث بوضوح التفاعل المعقد بين المجالات الكهربائية وتأثيرها العميق على آليات الاستخراج والتسارع التي تحكم حزم الإلكترون داخل تجاويف المسرع. من خلال التحليل الدقيق، نتمكن من معرفة التأثير المباشر للمجال الكهربائي، في ظل ظروف مختلفة داخل المحقن الضوئي مثل: طور التردد اللاسلكي، والذي بشكل مباشر يؤثر على كفاءة وجودة توليد الحزمة واستخراجها وعمليات التسارع اللاحقة داخل هذه التجاويف المتخصصة.

تتم هذه الدراسة البحثية بدعم واستعانة مباشرة باستخدام النماذج التحليلية وبرنامج المحاكاة "ماتلاب".

وتعتبر هذه الدراسة فريدة من نوعها أيضًا في البلاد حيث تفتح الافاق للوصول العلمي والموارد لعلماء الفيزياء والخبراء والباحثين في مجال المسرعات الجسيمية.

Introduction

Nowadays, particle accelerators have become important machines in high energy physics. These machines have been used much in wider fields, such as science, medicine, and industry at multiple length scales ranging from the sub-atomic (the realm of particle physics) to the anatomic level. The first accelerator dates to prehistoric-historic times, when men-built bows and arrows for hunting. The race to build modern particle accelerators began in 1911 when Rutherford discovered the atomic nucleus by scattering -particles off gold foil. These activities produced a series of innovative ideas such as the voltage rectifier (Cockcroft-Walton) and the Van de Graaff DC accelerators, the RF lines accelerators, the classic cyclotrons, the betatrons, the separate sector cyclotrons, the synchrotrons, and eventually storage rings and colliding beams. These accelerators can either be designed as linear accelerators or circular machines depending on the particles being accelerated and applications. In this technology, charged particles are emitted from either ion source (in the case of protons or heavy ions) or from electron guns which is the cathode. Presently, these instruments are extensively employed across various domains, as elaborated in the subsequent section, encompassing fields such as science, medicine, and industry, spanning multiple scales from the sub-atomic to the anatomical level. As shown in Figure 1, illustrates the development of this technology over the world for various kinds of accelerators since 1930s, and shows the upgrade of the beam energies from few handers of Kevs up to thousands of Tevs.

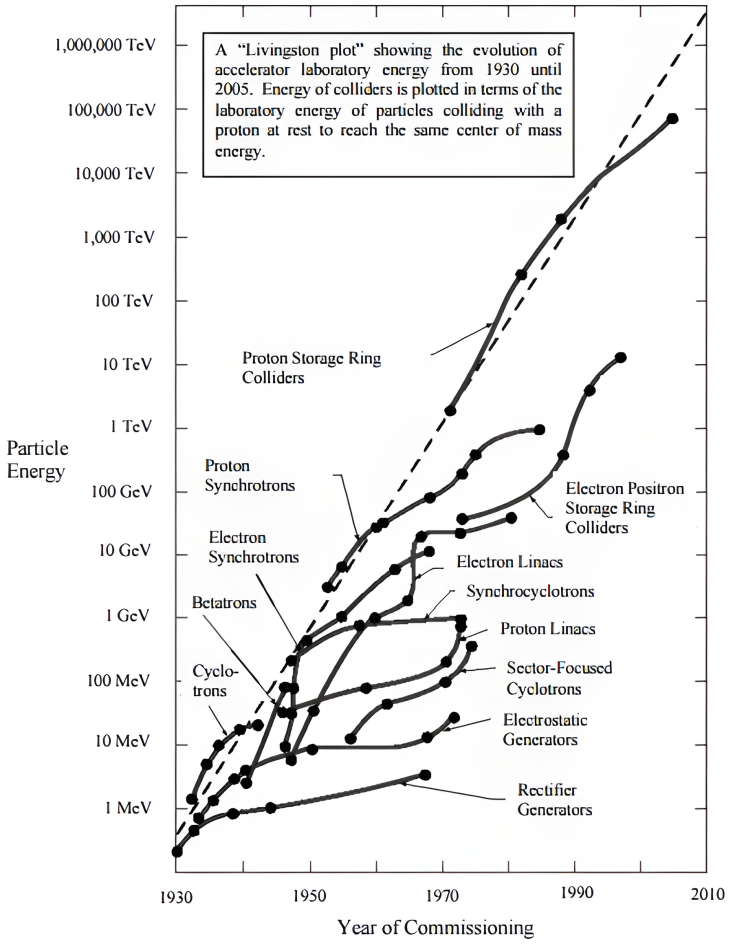

Figure 1: The development of high-energy accelerators labelled with technological progress.

As a part of particle accelerator studies, we will focus in this research on the following objectives to cover three main chapters. The first chapter describes particle accelerators in terms of their types and their applications. The second chapter describes the generality of a Standing Wave (SW) Radio-Frequency (RF) accelerator or as known as known an (RF) photo-injector. The third chapter will present the essential parametric simulation results using MATLAB with analytic models.

In this context, the objectives of this chapter can be succinctly outlined as follows:

- Analyzing the longitudinal profile of the standing electric field (E_z) inside the RF photo-injector accelerator at different RF phase configurations.

- Studying the dependency of the work function (Wi) of the cathode

material on the electric field (Ez).

- Investigating and clarifying the relation between the actual (RF) phase and the effective accelerating phase and their dependency on different electric field amplitudes.

- Simulating the electron kinetic energy at different RF phases with monitoring its ramping up through the accelerator length.

Chapter 1

Particle Accelerators

1.1 Introduction

The years around 1930s were essential time for the invention and building of particle accelerators. This has allowed physicists to utilize high-energy charged particle beams in many topics of physics e.g. to study the inner workings of matter at the scale of nuclei. This then opened the window for the development of particle accelerators and its underlying principles, which has its basis on the theoretical and experimental progress in fundamental physical phenomena. While substantial experiments with active particle accelerators beginning only in the twentieth century, their success depended on a fundamental physical knowledge of electromagnetic processes, which was primarily investigated through experimental and theoretical studies in the nineteenth and early twentieth centuries. The physics and technology of accelerators involves many branches of science, including electromagnetism, solid-state properties of materials, atomic physics, superconductivity, nonlinear mechanics, spin dynamics, plasma physics, quantum physics, radio-frequency, and vacuum technology. Accelerators have offered many useful applications as they can be used in nuclear and particle physics research, in industrial applications such as ion implantation and lithography, in biological and medical research with synchrotron light sources, in material science and medical research with spallation neutron sources, etc. Accelerators have also been used for radiotherapy, food sterilization, waste treatment, etc [4].

There exist a variety of particle accelerators that utilize diverse technical concepts and methodologies. The two basic classes of accelerators: electrostatic and electrodynamic (or electromagnetic) accelerators.

The foundation for all these accelerators lies in the interplay between static and dynamic electromagnetic fields and electric charge. Every type of particle accelerator emerges as a technical manifestation of these intricate interactions. From static electric fields to alternating current (AC) magnetic fields in betatrons, to radio frequency fields spanning from megahertz (MHz) to gigahertz (GHz) frequencies, electromagnetic fields are harnessed across a broad spectrum of frequency ranges. Moreover, there is ongoing exploration into innovative approaches such as particle acceleration using laser beams to achieve high-field strengths. This chapter will cover the history of the development, as well as working mechanisms, and applications for each type of particle accelerators: Electrostatic, Linear and Cyclotron accelerators [6].

1.2 Electrostatic Accelerator

In this scenario, the potential difference between two electrodes is utilized to accelerate charged particles forward, as depicted in the accompanying Figure1.1 . The full high voltage is distributed among several tubes yielding a stepwise acceleration of the beam.

As a rule of thumb,the electric field at the surface of polished stainless-steel electrodes in a high vacuum must not exceed 100 kV/cm. Higher fields cause violent discharges due to the emission and acceleration of electrons at the electrode surface.To avoid distortions of the ion trajectories by charge islands on the isolator walls the accelerating tubes should be overlapping such that an ion cannot 'see' the isolator walls [6].

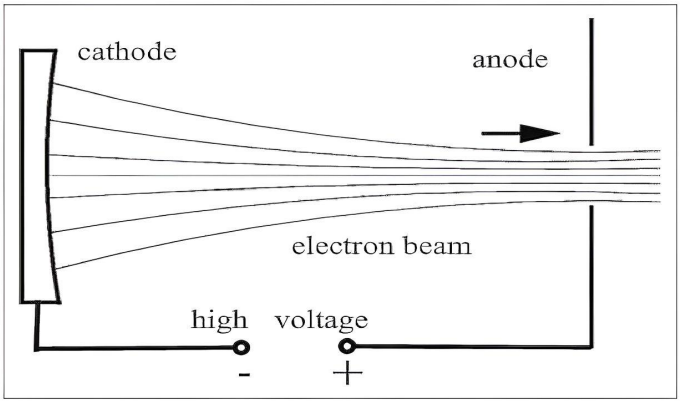

Figure 1.1: The principle of electrostatic accelerators.

This is of great importance in view of the low electric rigidity of low

energy ions. Similarly, the metal electrodes must be free of oil, hydrocarbon deposits and all kind of insulating deposits.In another, more modern application, electrons are accelerated by high electrostatic fields to produce intense x-ray after striking a metal target for use in medicine and industry.And the most famous example of such an accelerator is Van de Graaf. The next will briefly show the details of its mechanism. The first belt-charged electrostatic generator was developed by R. J. Van de Graaff in 1931. The Van de Graaff generator is made up of a motor-driven belt (made of rubber, vulcanized fabric or another flexible insulating material) stressed between two rollers (pulleys), an insulating column and a spherical or rounded high-voltage terminal electrode which is installed on top of the insulating column as shown in Figure 1.2. The belt is electrically charged by a brush or comb of metallic wires which is connected to a DC voltage source. The amount of electric charge sprayed on to the belt is controlled by the voltage Uc. The charge, which can be negative or positive depending on the polarity of the source, is carried by the belt to the terminal electrode. If the entire system is placed into high pressure vessel, filled with an electrically inert gas like Freon, voltages as high as 20 million volts can be reached. Such high voltage can be used to accelerate as well as protons or ions. High electrostatic voltages from a Van de Graff generator cannot be applied directly to only two electrons as shown in Figure 1.2, hence, to prevent voltage breakdown [3].

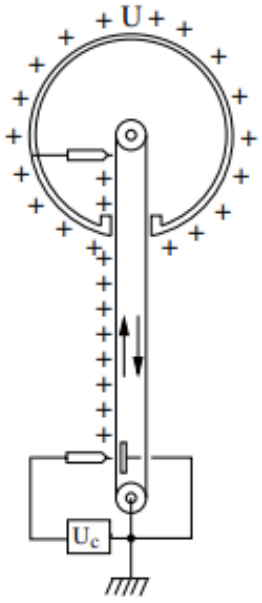

Figure 1.2: Scheme of the Van de Graaff generator.

The Van de Graff accelerator is still usable in much research in nuclear physics for a large variety of ion beams with an energy of 100 Kev up to 100 Mev. Besides that, it still used in many applications such as [3]:

Materials modification:

. Ion implantation and ion beam mixing.

Materials analysis:

. particle induced gamma ray emission (PIGE).

Particle production:

. Medical, security.

Radiation production:

. X-ray imaging.

1.3 Linear Accelerator

In a linear accelerator (LINAC) charged particles acquire energy moving on a linear path, their characteristic feature is that particles pass only once through each of the accelerating structures. As the Figure 1.3 shown. Another definition may be LINAC is a system that allows to accelerate charged particles through a linear trajectory by electromagnetic fields [1].

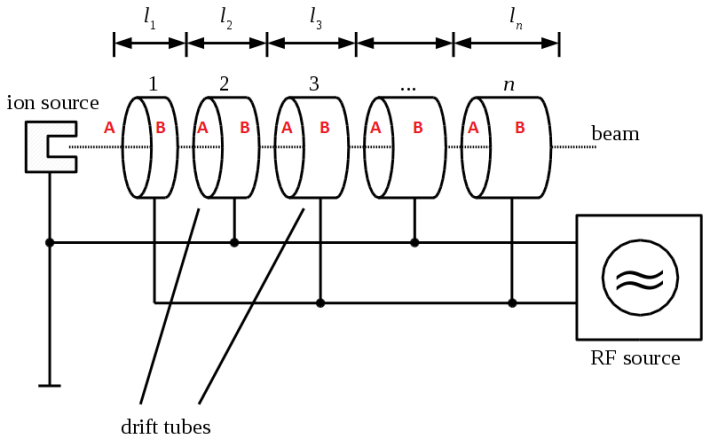

Figure 1.3: An example of a linear accelerator.

In the year 1924, Gustaf Ising, a Swedish physicist, proposed accelerating particles using alternating electric fields, with "drift tubes" positioned at appropriate intervals to shield the particles during the half-cycle when the field is in the wrong direction for acceleration. The voltage pulses arriving sequentially at the drift tubes produce accelerating fields in the

sequence of gaps, as the particle gain speed while the frequency remain constant, the gaps must space farther and farther to ensure the particles seeing a voltage applied once reaching each gap. But Ising was unable to demonstrate the concept. In 1928, Rolf Wideroe for his PhD thesis Wideroe built and demonstrated a simple linac, which had one drift tube between two accelerating gaps. He used a 25 Kev vacuum tube oscillator. This invention was a success in accelerating only once by the energy of 50 Kev, twice the applied voltage [7].

Both these designs were limited in the voltage sources available at that time until 1931 when the lead Luis Alvarez designed a proton drift-tube linac 12-m long, 1-m diameter, 4 MeV to 32 MeV, initially using surplus 200-MHz vacuum tubes. In contrast to the Wideroe type, an Alvarez LINACs applies RF power throughout the whole resonant chamber [1]. The early Alvarez-type LINACs lacked a robust mechanism for beam focus, leading to limitations in length and energy. Research on the strong focusing principle in the early 1950s paved the way for the incorporation of focusing quadrupole magnets inside drift tubes. This advancement allowed for the construction of longer and more powerful LINACs [8]. Today, advancements in accelerator technology have led to the rapid development and enhancement of accelerator designs, allowing them to achieve high energies up to the GeV range. The Stanford Linear Accelerator Center (SLAC) is the largest linear accelerator, spanning about 3.2 kilometers (2 miles) and can propel electrons to energies as high as 50 GeV. Situated in Menlo Park, California, United States, SLAC functions as a federally funded research and development center, currently supported by the United States Department of Energy and overseen by Stanford University [9]. Linear accelerators find diverse applications across various sectors, including but not limited to [10]:

Security:

. Cargo Scanning.

Medical Imaging and Treatment:

. X-Ray Radiation-therapy.

. Proton and Ion Therapy.

. Equipment Sterilization.

Industrial uses of accelerators:

. Ion Implantation.

. Food Irradiation.

1.4 Cyclotron Accelerator

The best known and one of the most successful devices for acceleration of ions to millions of electron volts is the cyclotron, which was invented by E. O. Lawrence in 1929. The first working model produced 80-keV protons in 1930. And about 140 of them are still in use around the world. About 50 cyclotrons have been completed since 1980 or are under construction. This shows that, although cyclotrons cannot accelerate particles to as high energies as can synchrotrons, much can be achieved with beams from cyclotrons both in physics and in other applications [11].

The term circular accelerator refers to any machine in which beams describe a closed orbit, thus all circular accelerators have a vertical magnetic field to bend particle trajectories and one or more gaps coupled to inductively isolated cavities to accelerate particles [12].

And the main characteristic of resonant circular accelerators is synchronization between oscillating acceleration fields and the revolution frequency of particles. The Figure 1.4 show that a cyclotron, as well as a linac, uses multiple acceleration by a radio frequency electrical field. However, the ions in a cyclotron are constrained by a magnetic field to move in a spiral path. The ions are injected at the center of the magnet between two semicircular electrodes called "Dees". As the particle spirals outward it gets accelerated each time it crosses the gap between the Dees. The time it takes a particle to complete an orbit is constant, since the distance it travels increases at the same rate as its velocity, allowing it to stay in phase with the RF. As relativistic energies are approached, this condition breaks down, limiting cyclotrons in energy [11].

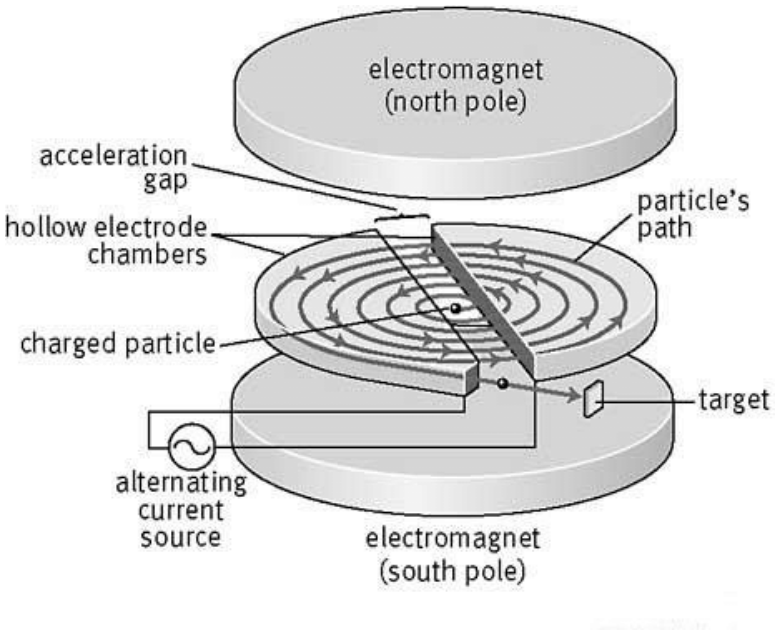

Figure 1.4: A schematic diagram of a Cyclotron.

This form of accelerator finds utility in various applications, such as [13]:

- Study of proton induced radioactivity in different matrials.
- A cyclotron as a spectrometer.
- Material research with beams at cyclotron energies.

Chapter 2

Longitudinal electron beam dynamics of an RF photoinjector

2.1 Introduction

This chapter briefly presents the longitudinal electron beam dynamics in the RF photoinjector in terms of its characterization, working principle, components and its applications.
Historically, photo-cathode RF guns or as called "photoinjectors" have served as the initial stage for generating and accelerating electron beams in particle accelerators working at different frequencies (from a few hundred MHz up to several GHz) depending on the different applications. In 1983, there were only 1 or 2 RF gun projects using such technology, but by 1990 there were more than 25 laboratories along with a few companies actively building and testing guns.
The photoinjector accelerator is typically composed of a laser-generated electron source, succeeded by an electron beam optical system that maintains and aligns the beam into a high-energy accelerator, as illustrated in the Figure 2.1. It consists of a cathode fabrication and/or transport system and electron gun, powered by RF or biased at a high voltage, beam optics for transporting and matching the beam to the high-energy accelerator, and assorted diagnostics, and controls. Basically, the electron beam quality is specified in terms of three quantities: Emittance, peak current and brightness.

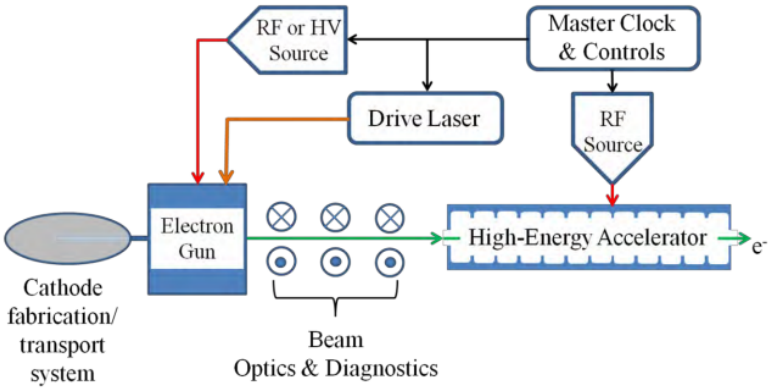

Figure 2.1: The parts of a photoinjector.

The photocathode may consist of a metal or one of various semiconductor materials. The gun options include a high voltage DC gun, a normal conducting RF (NCRF) gun, or a superconducting RF (SCRF) gun. It is crucial to match the drive laser with the cathode type and the desired pulse format [15].

The cathode laser beam, upon being conveyed to the vacuum section of the gun, undergoes reflection from the vacuum mirror. This reflection results in the generation of a photo-electron bunch upon striking the surface of the photocathode situated within the RF cavity. Subsequently, the electron bunch is produced once receiving sufficiently enough energy to escape from the cathode material then being accelerated by the RF fields and effectively focused through the synergy of static magnetic fields emanating from the focusing and bucking solenoids. At the conclusion of this process, the beam exits from the RF photoinjector with an energy level of approximately few MeVs, achieved through an input peak RF power of few MWs.

For efficient energy delivery to the electrons, the RF fields utilize the π-mode configuration. In this setup, the fields are orchestrated to alternate between acceleration and deceleration within adjacent cells, maintaining a 180' phase difference. As electrons are emitted from the cathode, they initially accelerate within the first half cell. The length of this segment is precisely calibrated so that as the electron progresses towards the subsequent cells, the field polarity changes, propelling the electron deeper into the cell for continued acceleration "synchronism condition" to avoid falling into decelerating fields thus, preventing the back components from the occurrence of breakdown events which are seriously hazardous [14]. Using the π-mode in RF fields for the electron beam acceleration can offer the

following advantages:

- Efficient Energy Transfer: Alternating between acceleration and deceleration in adjacent cells enhances energy transfer to electrons due to the relatively high shunt impedance in such mode.
- Improved Beam Quality: Controlled acceleration and deceleration phases maintain beam stability and quality.
- Reduced Beam Emittance: Helps minimizing beam divergence, resulting in better beam focus.
- High Acceleration Efficiency: Continuous acceleration throughout the cell structure maximizes efficiency.
- Enhanced Energy Spread Control: Allows for better control over the energy spread of the accelerated beam.
- Optimized RF Power Usage: Efficiently alternating phases helps optimizing RF power usage for effective energy delivery.

In general, the main advantage of choosing such photocathode is that the electron duration can be identified by the duration of the incident laser pulse, which can be in a pico-second or even tens of femto-second range. The photocathode RF guns combine the advantages of RF technology in comparison with other electron gun types. They can thus provide a high quality beam i.e. high energy few MeVs, short duration in ($\approx$ 100 fs, a high charge (up to 10 nC) in one bunch, low energy spread (approx. 0.1% rms) and low normalized transverse emittance (a few π.mm.mrad). It also has a benefit of a compactness of its size therefore, does not require a large lab-scale to be integrated which in turns reducing construction cost. The achievement of such properties is not available with the other electron sources. However, a disadvantage of such accelerators is the complexity of their mechanical design due to the need for both cooling and vacuum systems which have to be connected in a relatively short beam line in addition to the optical equipment. These points make it harder as the guns getting shorter as well as oscillating with higher frequencies. Currently, such technology is utilized as electron sources for different applications requiring a high electron bunch charge in addition to a high brightness electron beam, as is the case for X-ray free electron lasers such as LCLS project at Stanford laboratory in USA, ThomX at IJCLab in France laboratory FLASH at Desy and the European XFEL in Germany [16].

2.2 The longitudinal Electric Field and SW RF-photoinjector

The longitudinal field profile is described by the following equation, representing a standing wave pattern that characterizes the field distribution along the accelerator structure.

$$E_z(\varphi_0) = E_{max} cos(kz) sin(wt + \varphi_0) \tag{2.1}$$

where, E_{max} is the amplitude "maximum" electric field (MV/m), k is the wave number (ω/c) with ω is angular frequency 2πf (rad/s), f is the RF frequency (Hz) and c is the speed of light (3×10^8 m/s), z is the length of the photoinjector and φ_0 is the actual RF phase. From this expression, electrons see a longitudinal electric field of E_z at its maximum which is when z=0 at the photocathode surface, and when the RF phase of φ_0=90° (crest of the wave). This fact leads to the consideration of thermal stress on the cathode surface which can provide an advantage for the electron generation.

2.3 The Schottky Effect in RF photoinjectors

As to allow emitting electrons from the cathode surface, incident laser pulses must have an energy higher than the work function of the cathode material "electron tunnelling".

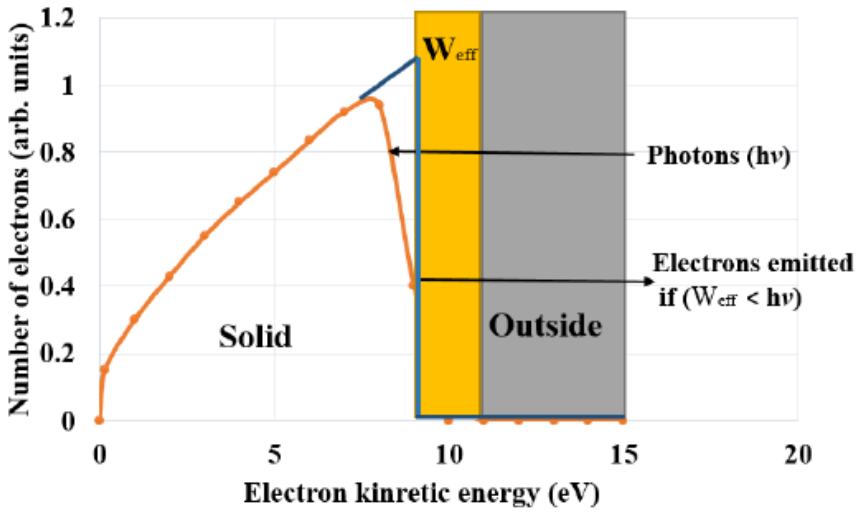

Figure 2.2: Schematic diagram of the electron emission from material.

The presence of a high electric field on the surface of the photocathode

leads to a decrease in the work function (W_i) of the cathode material. This reduction in the work function (δW) of the cathode, and it is known as the Schottky effect, enhances electron emission from the cathode. The Schottky effect can be quantified using the following formula:

$$\delta W = \sqrt{\frac{eE_z(\varphi_0)}{4\pi\varepsilon_\circ}} \tag{2.2}$$

where, δW is the reduction in the work function of the cathode, e is the electron charge, ϵ_0 is the dielectric permittivity of vacuum, which equal to 8.85^{12} (F/m) and E_z is descried in Equation 2.1 [14].

2.4 RF phase difference (slipping phase)

For the analytical modeling technique, the Kim-model is utilized to estimate the kinetic energy of electrons. These electrons are emitted from zero velocity to to very high velocity. The variation in two different velocity regimes makes it a bit challenging to derive the kinetic energy, taking also into account the phase slippage caused by the velocity difference between the oscillation of the wave inside the cavities and the low velocity of the electrons. This impact become dominant at the first stage of acceleration. Therefore, the observed discrepancy in the RF phase arises from the difference in velocity between the initial RF phase and electron velocity. Once the electrons see high enough electric fields, they become almost relativistic thus, the impact of the phase slippage "phase difference or phase variation" become less and less. For this reason, it is necessary to apply sufficiently high electric field as well as right RF phases to reduce the phase slippage and the falling into decelerating fields where the latter causing the lose of the electron beam. The effective RF phase φ_z that seen by electrons and directly involved in acceleration process can by expressed as:

$$\varphi_z = \varphi_0 + \frac{1}{2\alpha sin(\varphi_0)}(\sqrt{(\gamma_0 + 2\alpha k sin(\varphi_0)z)^2 - 1} - 2\alpha k sin(\varphi_0 z) - \gamma_0 + 1) \tag{2.3}$$

where $\alpha = \frac{eE_{max}}{2m_e c^2 k}$ and it plays a crucial role in indicating the strength of the accelerating field within an RF photoinjector. This parameter not only signifies the intensity of the field but also reflects the dynamics of electron acceleration as they traverse the system [16].

2.5 Kinetic energy of electron beam

Moreover, by considering the constancy of the effective accelerating phase φ_z, which experiences a gradual variation in the region far from the photocathode, an approximation of γ (where γ represents the Lorentz relativistic factor of the electron) can be derived. This approximation is expressed as [16]:

$$\gamma_z = \gamma_0 + \alpha(ksin(\varphi_z) - \frac{1}{2}cos(\varphi_z) - cos(\varphi_z + 2kz)) \tag{2.4}$$

The kinetic energy of the electrons can be readily expressed as:

$$E_{kin} = (\gamma_0 - 1)m_e c^2 + \alpha m_e c^2(ksin(\varphi_z) + \frac{1}{2}cos(\varphi_z) - cos(\varphi_z + 2kz)) \tag{2.5}$$

This expression shows that if needed to gain higher energy one has to play with several factors such as: increasing the amplitude of the electric field and/or choosing the suitable RF phase or either designing longer accelerator structure or designing a structure of a higher RF frequency.
Next chapter will present several simulation results of the previous crucial parameters considered in RF accelerator technology [14].

Chapter 3

Results and Discussion

3.1 Visualizing and Analyzing Data Using MATLAB

This chapter focuses on the advanced visualization and analysis of phenomena in 1.5 cell standing wave RF photoinjectors using MATLAB program. Begin with examining the electric field profile in SW RF photoinjector by visualizing the electric field distributions. Next, Schottky effect, through graphical representations aiming to elucidate the impact of the electric field to apply Schottky effect on electron emission efficiency within the Rf photoinjector. Also, analyzing the RF phase differences (slipping phase), to illustrate how phase variations affect synchronization and energy gain in the photoinjector. Finally, the kinetic energy profiles of electron beams as they traverse the photoinjector, and by plotting these energy distributions, it will be clear to evaluate the effectiveness of the acceleration process as well as identify the potential areas for improvement.

Throughout this chapter, MATLAB program is used to create detailed graphs and plots, enabling clear interpretation of complex data. These visualizations enhance the understanding of RF photoinjector.

The figure 3.1 shows the sequential process of the Kinetic energy function concerning the initial RF phase. This function was a focal point of this research within the "Simulation of Electron Beam Kinetic Energy" section 3.5.

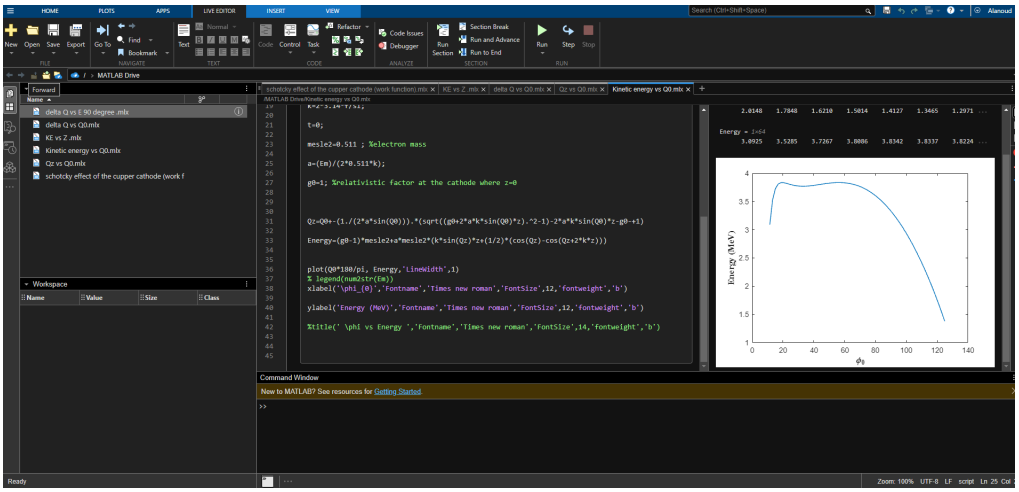

Figure 3.1: MATLAB Window: Research Function Analysis.

When observing the editor window in the middle, you can input MATLAB scripts. The Workspace window on the right showcases all variables currently stored in MATLAB's memory. On the left, the Current Folder window exhibits files within your directory. To execute a script, use the green run button from top to bottom. For creating, saving, exporting, or opening script files, utilize commands on the toolbar [17].

3.2 Electric field profile in a SW RF photoinjector

Figure 3.2 shows the electric field profile on the (1.5 cell working at S-Band of 3 GHz), where E_{max}=100 (MV/m), along a photoinjector with the length of z= 0.08 (m) at various initial RF phases (0, 45°, 90°, 225°, 270°). The influence of the RF phase on the electric field along the photoinjector is clearly observable. At ϕ_0=0, sin (0) equal zero therefore, E_z equals zero, which means no acceleration occurs, while at ϕ_0 =90° and 45° the E_z is accelerating field and specially at z=0 as well as at ϕ_0 =90°, the maximum electric field is seen because E_z=E_{max}. When ϕ_0=225° and 270°, E_z is decelerating field which forces the emitted electrons to travel toward the cathode, and this may cause damage the components behind if the electron charge is relatively high. Thus, the caution has to be taken into account to avoid such breakdown of the whole system by choosing the right RF phase region [14].

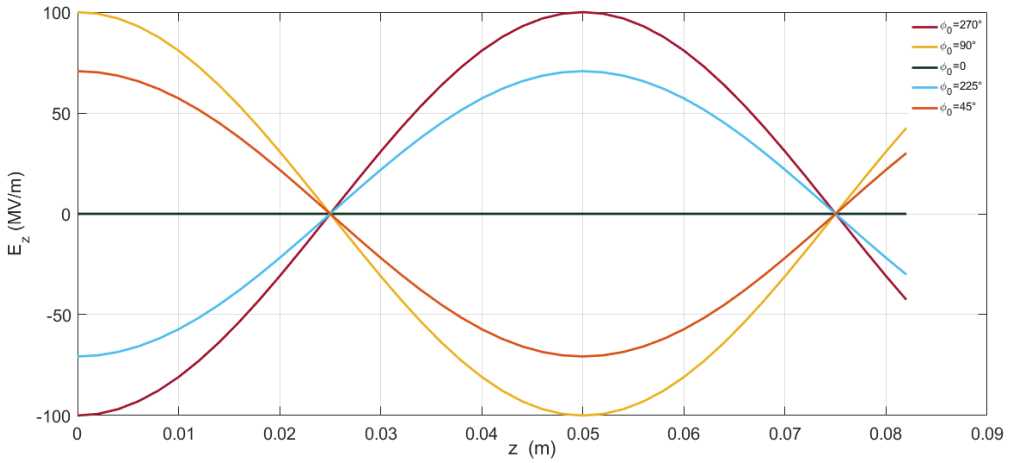

Figure 3.2: The electric field Ez along the photoinjector at different RF phases.

3.3 Electric field effect on the cathode material "Schottky effect"

Figure 3.3 shows the reduction in the work function of different cathode materials namely, Copper (Cu), Lead (pb) and Magnesium (Mg). Their initial work functions W_i are 4.4 eV, 4 eV and 3.6 eV respectively as a function of the accelerating electric field E_z ranging from 0 to 100 MV/m on the cathode surface (z=0). W_i is linearly reduced as E_z increases (inversely proportional) up to δW around 0.38 eV. This reduction in the work function allows emitting more electron charges in the lab, and this effect can be seen in the experimental test presented in Ref [14], where the electron charge emission increases from 30 pC to 110 pC.

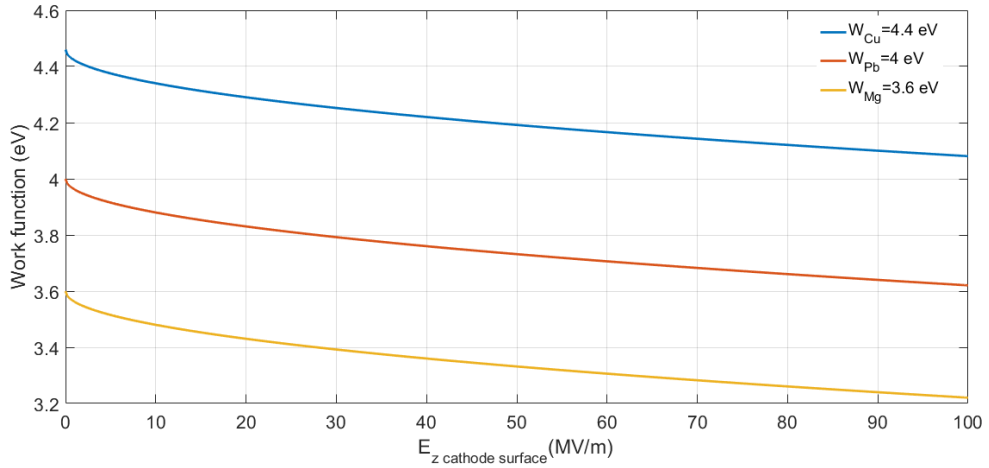

Figure 3.3: The resulting work function of the cathode (Cu, Pb and Mg) as a function of the accelerating electric field E_z on the cathode surface (z=0).

3.4 RF Phase difference due to the velocity variation

Figure 3.4 shows the relationship between the effective accelerating RF phase φ_z , seen by electrons, and the initial RF phase φ_0 ranging from between 0 to 180° at different E_{max} values (100 MV/m, 90 MV/m, 80 MV/m). General view, as the electric field gets higher we notice that φ_z has lower effect. This is noticeable as the electric field is high enough, electrons will overcome the slippage with lower degrees in difference in the other words, the electrons are well accelerated and traveling with almost close to the speed of light "relativistic".

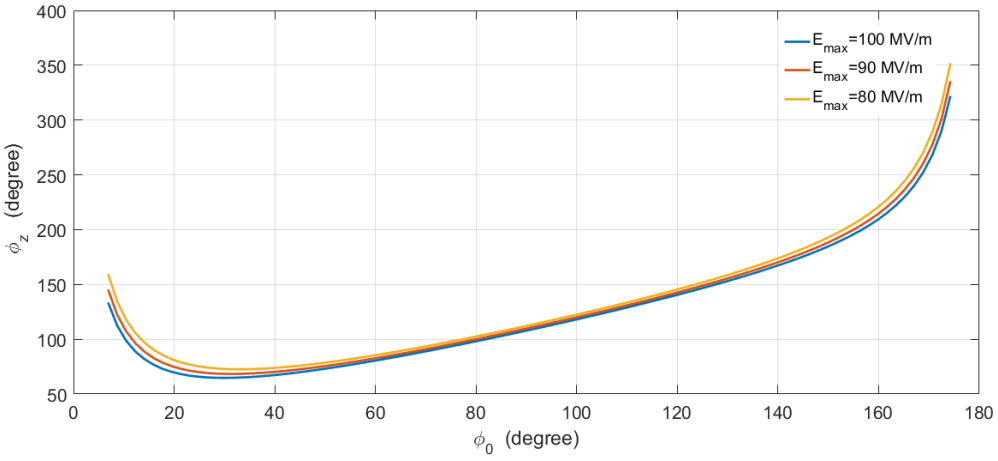

Figure 3.4: The effective accelerating phase (φ_z), seen by electrons, as a function of the actual RF phase (φ_0) for different E- fields.

Figure 3.5 shows the effective accelerating phase (φ_z), seen by electrons, as a function of the photoinjector length for different E-fields at the initial RF phase of 90°. It is noteworthy that the acceleration phase φ_z exhibits a gradual variation with increasing distance (z) from the photocathode. When electrons are emitted close to the photocathode, the accelerating phase φ_z presents an increase for all fields with lower increase for the higher fields. As the electrons get far from the cathode region, they reach relativistic speeds thus, the phase φ_z stabilizes more rapidly, particularly in regions characterized by higher field strengths. This stabilization marks a transition towards a more consistent and synchronized interaction between the electrons and the accelerating field. As electrons travel a few centimeters away from the cathode, they begin to achieve synchronization with the accelerating field ,and this implies that the electrons slipping on RF field is predominantly confined to the cathode region [14].

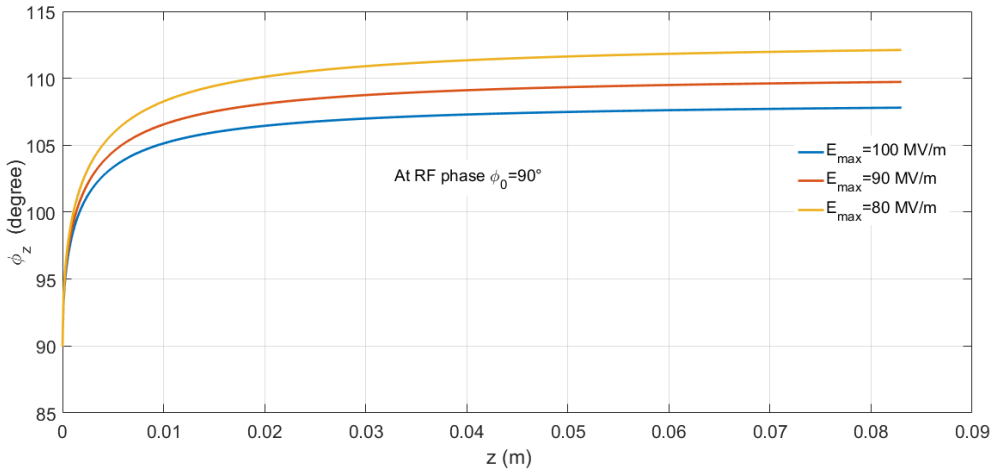

Figure 3.5: The effective accelerating phase (φ_z), seen by electrons, as a function of the photoinjector length for different E-fields at the initial RF phase of 90°.

Figure 3.6 represents the RF phase difference as a function of the actual "initial" RF phase (φ_0) at the same E- fields. As can be seen, the minima for all fields locate between 80° and 100° and of course, lower for higher fields.

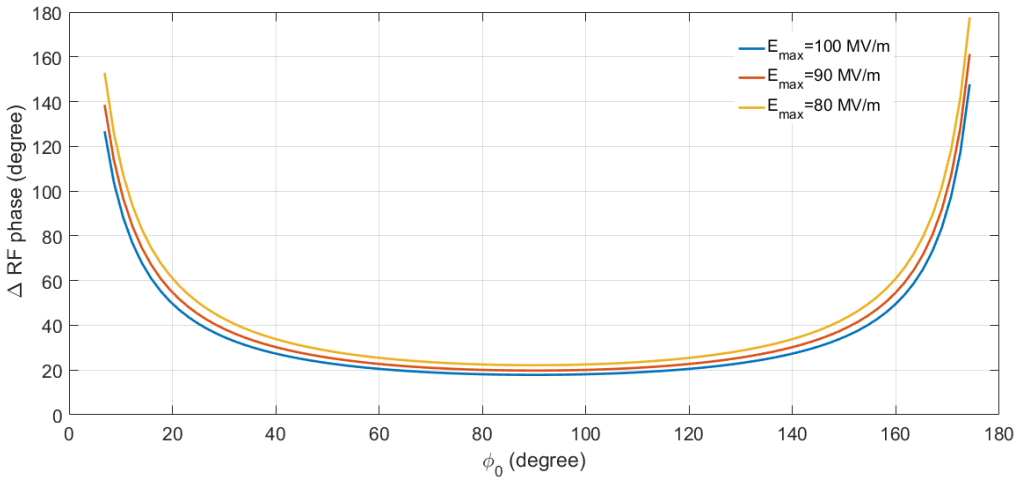

Figure 3.6: The RF phase difference (φ_z-φ_0) as a function of the actual "initial" RF phase (φ_0) at different E_{max}- fields.

Once again, Figure 3.7 shows the RF phase difference as a function of the maximum electric field ranging between 20 MV/m to 120 MV/m at different initial RF phases φ_0 (45°, 90°, 120°). As previously mentioned that the phase difference influence can be reduced through increasing the longitudinal electric field E_z and this can be fulfilled by increasing the maximum E_{max} and/or choosing better initial Rf phase φ_0. The phase difference Δ RF, for example in the case of 90°, is reduced from 80° at 20 MV/m to around 20° at 120 MV/m. This preservs the acceleration efficiency without loosing the electron beam.

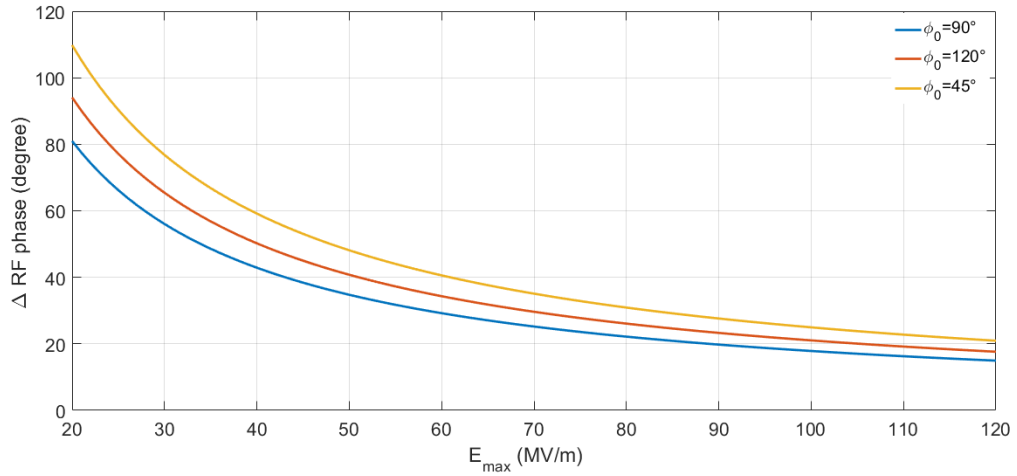

Figure 3.7: The RF phase difference as a function of maximum electric field E_{max} at different φ_0 (45°, 90°, 120°)

3.5 Simulation of electron beam kinetic energy

Figure 3.8 illustrates the final electron kinetic energy as a function of the initial RF phase φ_0 for different maximum electric field E_{max} (80 MV/m, 90 MV/m, 100 MV/m). It shows the dependency of the final kinetic energies on both E_{max} and φ_0. For E_{max}-100 MV/m, the maximum energy achieved is just around 4 MeV while for the E_{max} of 90 MV/m and 80 MV/m are 3.5 MeV and 3 MeV respectively. The maximum energies can be observed in the RF phase φ_0 region between 20° to 80°. By moving away from this region, the seen electric field E_z by electrons is being weaker witch in turns causing the electrons to gradually gain lower energies up to falling into decelerating fields. Thus, the electrons will be accelerated toward the cathode. For such reason, it is necessary to be careful when accelerating high electron current to avoid any case of breakdown of the entire system.

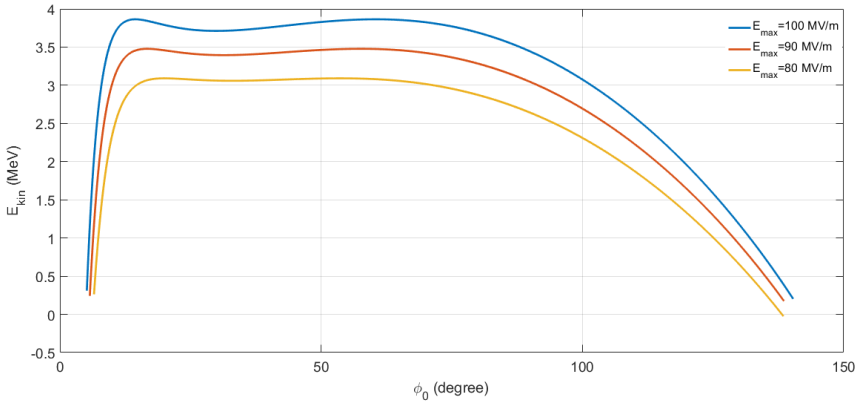

Figure 3.8: The electron kinetic energy E_{Kin} as a function of the RF phase φ_0

The Figure 3.9 shows the ramping up of the electron kinetic energy E_{Kin} along the photoinjector of 1.5 cell for different chosen values of E_{max} (100 MV/m, 90 MV/m and 80 MV/m) at an initial RF phase of 90°. The maximum energies at this RF phase for 100 MV/m, 90 MV/m and 80 MV/m are 3.5 MeV, 3 MeV and 2.5 MeV respectively at the exit (at z=8.3 cm). This emphasizes the excellence of such machine in accelerating electron beams to high energies (MeVs) in a relatively short distance in comparison with the classical accelerators.

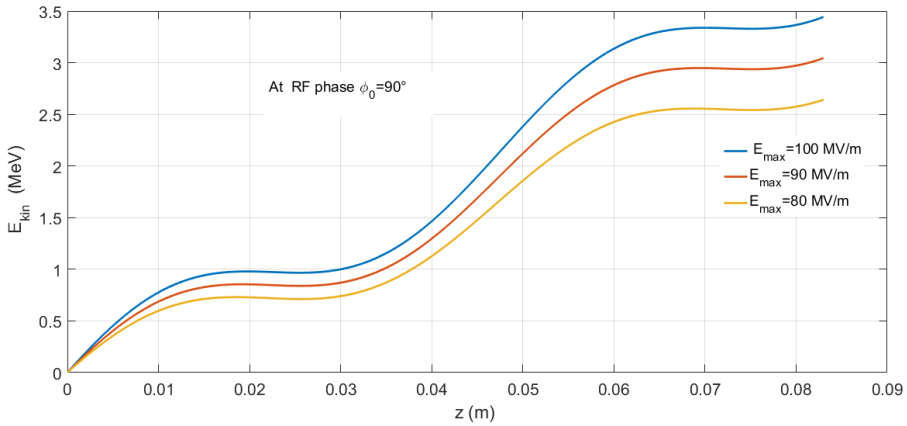

Figure 3.9: Ramping up of the electron kinetic energy E_{Kin} along the photoinjector for different E_{max} and at an initial RF phase of 90°.

It is obvious that when applications require higher energies and beam currents, it becomes necessary to adjust several parameters such as: the amplitude of the electric field and/or choosing the suitable RF phase or either designing longer accelerator structure or designing a structure of a higher RF frequency. At the same time, the cathode material is a crucial task to choose concerning its work function, electrical conductivity and cost. It should not also be forgotten the characteristics of laser system laser incident on the cathode material, which plays an important role in the photoinjector technology [6].

Chapter 4

Conclusion

This project has addressed three main chapters, beginning with an introduction and overview of the various types of accelerators, their invention, and their diverse applications. Also, provided a detailed discussion on the longitudinal dynamics on electron beam extraction and acceleration in SW RF photoinjector accelerator. And included simulations analytical models to examine the key principles and critical factors such as, work function, high electric fields, RF phase, and the kinetic energy of the electron beam. However, the research also identified several challenges associated with SW RF photoinjector in graphing their performance characteristics, and describing each type. Overall, this work underscores the importance of continued research and development in the area of RF photoinjectors and drive advancements in both fundamental science and practical applications.

References

[1] Wangler, T. P. (2008). RF Linear accelerators. John Wiley and Sons.

[2] Padamsee, H., Knobloch, J., and Hays, T. (2008). RF superconductivity for accelerators. John Wiley and Sons.

[3] Hinterberger, F. (2006). Electrostatic accelerators.

[4] Lee, S. Y. (2018). Accelerator physics (p. 568). World Scientific Publishing Company.

[5] Tavares, P. F. (2020). Brief Introduction to Particle Accelerators. arXiv preprint arXiv:2006.02821.

[6] Wiedemann, H. (1994). Particle Accelerator Physics. Physics Today, 47(7), 61.

[7] Rammohan, N., Randall, J. W., and Yadav, P. (2022). History of technological advancements towards MR-Linac: the future of image-guided radiotherapy. Journal of Clinical Medicine, 11(16), 4730.

[8] Lapostolle, P. M. (1989). Proton linear accelerators: a theoretical and historical introduction.

[9] Krejcik, P. (2013, January). The development of modern particle accelerators at the Stanford Linear Accelerator Center. In Journal and Proceedings of the Royal Society of New South Wales (Vol. 146, No. 449/450, pp. 91-102).

[10] Sheehy, S. (2024). Applications of Particle Accelerators. arXiv

preprint arXiv:2407.10216.

[11] Heikkinen, P. (1994). Cyclotrons.

[12] Kolomenskii, A. A., and Lebedev, A. N. (1966). Theory of circular accelerators. Wiley, New York.

[13] Dutto, G., and Craddock, M. K. (Eds.). (1993). Cyclotrons And Their Applications-Proceedings Of The13th International Conference, Vancouver, 1992. World Scientific.

[14] Alkadi, M. (2022). S-band electron LINAC for ThomX (Doctoral dissertation, Université Paris-Saclay).

[15] Dowell, D. H., and Lewellen, J. W. (2013). Photoinjector theory. An Engineering Guide To Photoinjectors, edited by T. Rao and DH Dowell (CreateSpace Independent Publishing Platform, 2013), 1.

[16] T. Vinatier. Influence of laser parameters on the relativistic short electron bunches dynamics in linear accelerators based on RF-guns and development of associated diagnostics. PhD thesis, Université Paris Sud-Paris XI, 2015.

[17] Matlab, S. (2012). Matlab. The MathWorks, Natick, MA, 9.

[18] Panofsky, W. K. (1997). Evolution of particle accelerators. SLAC Beam Line, 27(1), 36-44.

[19] Accelerators for society. (n.d.).`http://www.accelerators-for-society.org/about-accelerators/index.php?id=21`